Acta Med. Okayama, 2013
Vol. 67, No. 6, pp. 359–367

Acta Medica Okayama
http://escholarship.lib.okayama-u.ac.jp/amo/

Original Article

In Vitro Assessment of Factors Affecting the Apparent Diffusion Coefficient of Jurkat Cells Using Bio-phantoms

Kazunori Katashima[a], Masahiro Kuroda[b]*, Masakazu Ashida[a], Takanori Sasaki[c], Takehito Taguchi[b], Hidenobu Matsuzaki[a], Jun Murakami[a], Yoshinobu Yanagi[a], Miki Hisatomi[a], Marina Hara[a], Hirokazu Kato[b], Yuichi Ohmura[b], Tomoki Kobayashi[b], Susumu Kanazawa[c], Sosuke Harada[c], Mitsuhiro Takemoto[c], Seiichiro Ohno[d], Seiichi Mimura[d], and Junichi Asaumi[a]

Departments of [a]Oral and Maxillofacial Radiology and [c]Radiology, Okayama University Graduate School of Medicine, Dentistry and Pharmaceutical Sciences, [b]Radiological Technology, Graduate School of Health Sciences, Okayama University, [d]Central Division of Radiology, Okayama University Hospital, Okayama 700–8558, Japan

It is well known that many tumor tissues show lower apparent diffusion coefficient (ADC) values, and that several factors are involved in the reduction of ADC values. The aim of this study was to clarify how much each factor contributes to decreases in ADC values. We investigate the roles of cell density, extracellular space, intracellular factors, apoptosis and necrosis in ADC values using bio-phantoms. The ADC values of bio-phantoms, in which Jurkat cells were encapsulated by gellan gum, were measured by a 1.5-Tesla magnetic resonance imaging device with constant diffusion time of 30 sec. Heating at 42℃ was used to induce apoptosis while heating at 48℃ was used to induce necrosis. Cell death after heating was evaluated by flow cytometric analysis and electron microscopy. The ADC values of bio-phantoms including non-heated cells decreased linearly with increases in cell density, and showed a steep decline when the distance between cells became less than 3 μm. The analysis of ADC values of cells after destruction of cellular structures by sonication suggested that approximately two-thirds of the ADC values of cells originate from their cellular structures. The ADC values of bio-phantoms including necrotic cells increased while those including apoptotic cells decreased. This study quantitatively clarified the role of the cellular factors and the extracellular space in determining the ADC values produced by tumor cells. The intermediate diffusion time of 30 msec might be optimal to distinguish between apoptosis and necrosis.

Key words: ADC, apoptosis, necrosis, hyperthermia, cell density

Diffusion-weighted magnetic resonance imaging (DW-MRI) is frequently used in clinics, and is used for whole-body screening for tumors [1]. It is well known that many tumor tissues show lower ADC values. The low ADC values of tumor tissues might originate from several factors; *e.g.*, cell structure [2–4], membranous content, intracellular components, extracellular space [1, 5] and blood flow in tissues [6]. However, it is still unclear the degree to which each factor contributes to the lowering of ADC values. Recently, it has been reported that the diffusion time at the measurement of ADC is crucial; measured at

Received September 18, 2012; accepted July 26, 2013.
*Corresponding author. Phone:+81–86–235–6873; Fax:+81–86–235–6873
E-mail:kurodamd@cc.okayama-u.ac.jp (M. Kuroda)

different times, ADC reflects physically very different restrictions -- mainly cytoplasm (and possibly smaller intracellular structures) in the short term, and mainly cell membrane permeability in the very long term [7–8]. Besides, fractional analysis [9] for multi-components in the body has progressed to interpret the results of ADC with complete certainty. We previously reported a newly developed bio-phantom [10] containing gellan gum and living tumor cells, which can be imaged by clinical MR devices. It enables us to place cells uniformly at a given cell density in bio-phantoms. Gellan gum does not affect ADC values when used in bio-phantoms [10]. Besides, cells are not damaged by heat during the manufacture of these bio-phantoms, as cells are enclosed at room temperature [11]. Gellan gum has been reported as an optimal material for three-dimensional cell culture [11–12]. The cells can be cultured physiologically without increasing dead cells and swelling at isotonic condition, and can grow and undergo cell division in the gellan gum [11–12]. We applied this material as the bio-phantom for MR imaging [10].

Using these bio-phantoms, we previously found that extracellular space plays an important role in determining the ADC values of the bio-phantoms [10]. However, it remains unsolved how much the extracellular space actually contributes to the ADC values. Although several reports have examined ADC values *in vitro* using cultured cells [2, 10, 13–17], the exact assessment of the relationship between cell density and ADC values is impossible without the use of a bio-phantom [10, 15]. In this study, we examined ADC values using the bio-phantom with constant intermediate diffusion time, clarified the relationship among ADC values, the center-to-center distance of cells and the actual cellular density, and analyzed factors affecting ADC values, especially focusing on the role of the cell density, extracellular space and intracellular factors. Recently, it was reported that the ADC of tumors changes after chemotherapy due to apoptosis [18]. We also clarified that the intermediate diffusion time of 30 msec was optimal to distinguish between apoptosis and necrosis.

Materials and Methods

Cells and culture. We used a human lymphoma cell line, Jurkat, which was kindly provided by RIKEN (Ibaraki, Japan) for the present study, as our previous report clarified that Jurkat cells undergo apoptosis and necrosis following heating at 42℃ and 46℃, respectively [19]. The cells were cultured in RPMI 1640 medium (pH7.4; Gibco, Grand Island, NY, USA) supplemented with 10% fetal bovine serum (JRH Biosciences, Lenexa, KS, USA) and 1% penicillin-streptomycin-neomycin (15640–055, Gibco). Cell culturing was performed in an incubator with 5% CO_2 plus 95% air at 37℃. Rotational culturing was performed using spinner flasks (3153, Corning, NY, USA) on a magnetic stir plate (ULS-4, AS ONE Co., Tokyo, Japan) set at 15 rpm in an incubator under 5% CO_2 plus 95% air at 37℃.

The number of cells with diameters larger than 8 μm was measured with an electric cell counter (Coulter Electronics Ltd., Luton, UK) before each treatment of cells, because most of the Jurkat cells had diameters larger than 8 μm, with the average diameter being 9.6 μm [10].

Cell treatments.

1. Heating treatment Cells were heated at 42℃ for an hour in a water bath (Thermal Robo TR2, Iuchi Inc., Osaka, Japan) and were incubated at 37℃ for 9 h to induce apoptosis. Alternatively, cells were heated at 48℃ for an hour in a water bath and incubated at 37℃ for 5 or 24 h to induce necrosis.

2. The destruction of cell membrane by sonication Cells were treated 16 times for 9.9 sec each at 0℃ with 30 watts in a sonication device (Sonics & Materials Inc., Newtown, CT, USA) to break down the cellular structure.

3. Flow cytometric analysis The double staining method using enhanced green fluorescent protein-labeled Annexin V (AV) and propidium iodide (PI) to estimate the number of cells undergoing apoptosis and necrosis as described previously [19]. The stained cells were analyzed with a flow cytometer, FACSCalibur, and Cell Quest software (Becton Dickinson, San Jose, CA, USA).

Particle analysis was undergone by measuring the relative diameter of particles using the degree of forward scatter. We defined particles smaller than the control cells as micro-particles.

Summit software (BD Biosciences, San Jose, CA, USA) was used for these analyses.

4. Observation by scanning and transmission electron microscope The cells were fixed, stained, and

observed by scanning electron microscope (S-4800, Hitachi High-Technologies Co.) and an H-7650 transmission electron microscope (Hitachi High-Technologies Co.).

Encapsulation of cells into a bio-phantom. The cells were encapsulated into bio-phantoms according to the previously reported method [10]. In brief, the medium containing cells was concentrated to about 2 ml, and then moved into a micro cuvette (Halbmikro 1.5 ml, Greiner, Düsseldorf, Germany) (Fig. 1A). The medium in the cuvette was centrifuged at 1,500 rpm for 5 min and the supernatant was removed. Then, the cells were diluted by 0.5 w/w% gellan gum, which had been dissolved in distilled water and highly concentrated ($\times 10$) phosphate buffered saline (PBS), to yield a final concentration of 0.25 w/w% gellan gum in PBS. Cells were encapsulated in bio-phantoms at final cell densities between 3.0×10^7 and 1.2×10^9/ml. When cells were encapsulated at high cell densities of 6.0×10^8/ml to 1.2×10^9/ml, gellan gum was not added to the bio-phantom after the supernatant was removed from the centrifuge.

Measurement of the center-to-center distance of cells. Cell density was calculated using the number of cells. The center-to-center distance (2 r) of cells was calculated by a close-packing grid using the following expression: $2\,r = 2 \times (0.177/a)^{1/3}$, where a indicates cell density [20].

Measurement of ADC values by MRI.

1. Phantom container Up to 24 bio-phantoms were put into the phantom container which was filled with PBS. The phantom container including bio-phantoms was heated to 37℃ using a water bath. The phantom container and a heat-retention gel material were put into a home-made case of polystyrene foam to keep the phantom temperature at 36.5 ± 0.5℃ during MR imaging.

2. MR imaging MR images of bio-phantoms were taken by a clinical 1.5-Tesla MRI device (Achieva 1.5T, Philips Electronics Japan Co., Tokyo, Japan) and its head coil. Triaxial diffusion-weighted (DW) images were taken orthogonally with motion probing gradients applied in x, y, z directions by a multi-shot echo planar imaging sequence. The number of shots was set to 9. The scan parameters were set as follows: 2,000 msec of relation time, 100 msec of echo time, 100×100 mm field of view (FOV), 256×256 matrix, b values of 0, 250, and 500 sec/mm^2, and a thickness of 5 mm. All data were obtained at 30 msec of diffusion time (Δ), which was the interval between onsets of diffusion gradient pulses, 17.4 msec of the diffusion gradient pulse duration (δ), and 24.2 msec of effective diffusion time ($\Delta - \delta/3$). The amplitude, G of the diffusion gradient pulse varied from 0 to 30.9 mT/m. The triaxial DW images were taken with the phantom temperature at 36.5 ± 0.5℃.

3. Calculation of ADC values The isotropic DW image for each b value was created from triaxial DW images by calculation of the root-mean-square of signals at each pixel. ADC values were decided for each pixel of isotropic DW images by calculating the change rate of logarithms of signal intensities on isotropic DW images against b values using the least-squares method. An ADC map was made using the ADC values of each pixel on isotropic DW images. The mean ADC values of the bio-phantoms were calculated from square regions of interest on the ADC map ranging from 5×5 to 7×7 pixels (Fig. 1B) using Image-J software (National Institutes of Health, Bethesda, MD, USA).

Results

Double staining with AV and PI. The double staining with AV and PI revealed that the heat

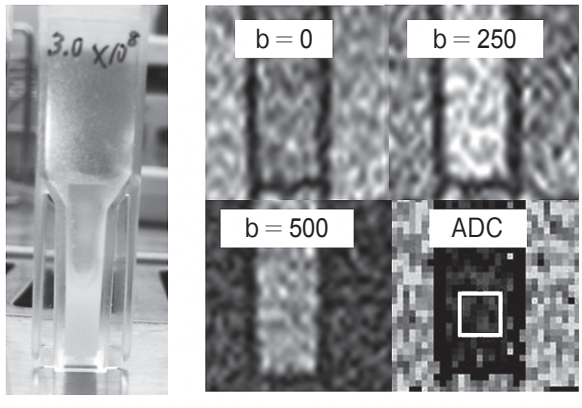

Fig. 1 The phantom and methods used. (A) Bio-phantom. (B) DW images and ADC map of the bio-phantom. Values of b = 0, 250 and 500 indicate the DW images taken with each b-value. The ADC indicates ADC map. The square on the ADC map indicates the region of interest that was used for the calculation of the mean ADC values.

treatment at 42℃ increased the number of apoptotic cells. The rates of early-stage apoptotic cells, stained by AV alone, were $13.2 \pm 18.2\%$ at 9h after heating at 42℃. The rates of total apoptotic cells including the secondary necrosis [19], stained with AV, were $21.7 \pm 12.0\%$ at 9h after heating at 42℃, compared to 1.3% of normal cells (Figs. 2A, B). The heat treatment at 48℃ for 1h increased the number of necrotic cells, which were stained by both AV and PI, with the prolongation of post-heating incubation time. The rates of necrotic cells were 59.6% and 97.9% after incubation for 5h and 24h after heating at 48℃, respectively, compared to 1.2% of normal cells (Figs. 2C, D, E and Fig. 3).

Observation by scanning and transmission electron microscope. Figs. 4A, B, C, G, H and D, E, F show cells observed with scanning electron microscope and transmission electron microscope, respectively. Budding appeared on the surface of cells at 9h after heating at 42℃ (Figs. 4B, E), compared with control cells (Figs. 4A, D). The inside of the budding extended into the cytoplasm. Micro-particles were observed in the extracellular space between the apoptotic cells (Fig. 4H). It is thought that micro-particles are apoptotic bodies. The cellular membranes that create apoptotic bodies seemed to have little damage. Heating at 48℃ made fine holes on the surface of cells (Fig. 4C), and ruptured the cell membranes (Fig. 4F) at 24h after heating at 48℃. Normal cellular structures were not observed because sonication destroyed the membranes and the membranous organelles of cells (Fig. 4G).

The relationship between cell density, ADC and the center-to-center distance of cells. Fig. 5 shows ADC values of bio-phantoms. The average ADC value of bio-phantoms which did not include cells was $3.06 \times 10^{-3}mm^2/sec$ compared to $3.03 \times 10^{-3}mm^2/sec$, that of PBS. The ADC values of bio-phantoms including normal cells (Fig. 5A) decreased linearly according to the increase in cell density and the decrease in the center-to-center distance of cells (Fig. 5F), when cell density was within the range of $3.0 \times 10^7/ml$ to $6.0 \times 10^8/ml$. When cell density increased into the range between $6.0 \times 10^8/ml$ and $1.2 \times 10^9/ml$, and the center-to-center distance of cells decreased to less than 13μm (Fig. 5F), ADC values showed a steep decline with sweeping form (Fig. 5A). The destruction of cell membranes by sonication increased the ADC values (Fig. 5B). The minimum ADC value of sonicated cells at the highest cell density was $2.36 \times 10^{-3}mm^2/sec$. The ADC values of sonicated cells decreased linearly with the increase in cell density. The reduction rate of ADC values of sonicated cells as a function of cell density was $-6.67 \times 10^{-7}ml\ mm^2/$

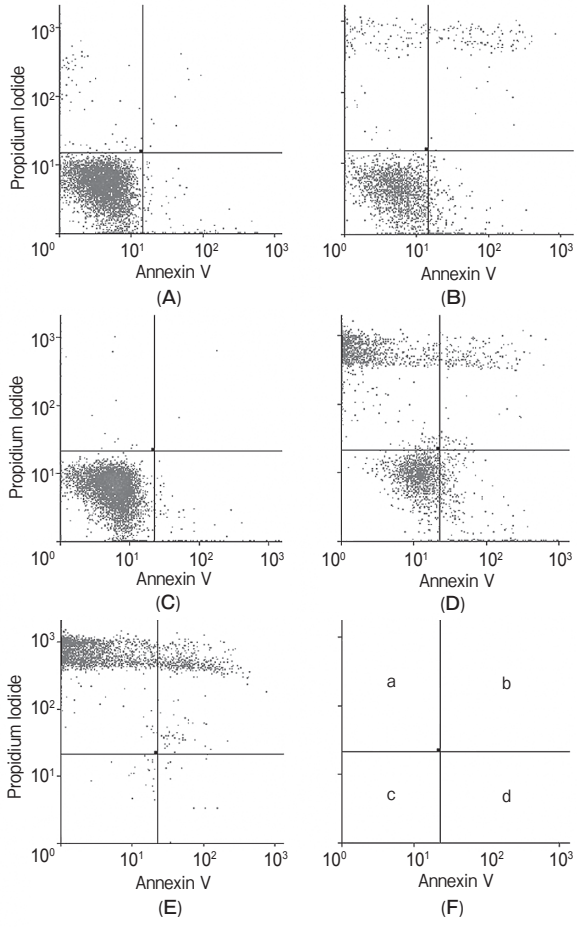

Fig. 2 The histogram of normal cells and heated cells at 42℃ and 48℃ stained with Annexin V and propidium iodide. (**A**) and (**C**) Normal cells. (**B**) Apoptotic cells incubated for 9h after heating at 42℃. (**D**) Necrotic cells incubated for 5h after heating at 48℃. (**E**) Necrotic cells incubated for 24h after heating at 48℃. The horizontal axis indicates the sensitivity for Annexin V. The vertical axis indicates the sensitivity for propidium iodide. (**F**) Areas a, b, c, and d indicate the following: a and b, necrosis; c, normal living cell; and d, early apoptosis. In graph (A), a = 0.69%, b = 0.08%, c = 97.70%, d = 1.53%. In graph (B), a = 14.05%, b = 4.77%, c = 72.88%, d = 8.29%. In graph (C), a = 1.74%, b = 0.43%, c = 95.68%, d = 2.15%. In graph (D), a = 67.13%, b = 3.53%, c = 24.29%, d = 5.05%. In graph (E), a = 91.47%, b = 7.98%, c = 0.36%, d = 0.20%.

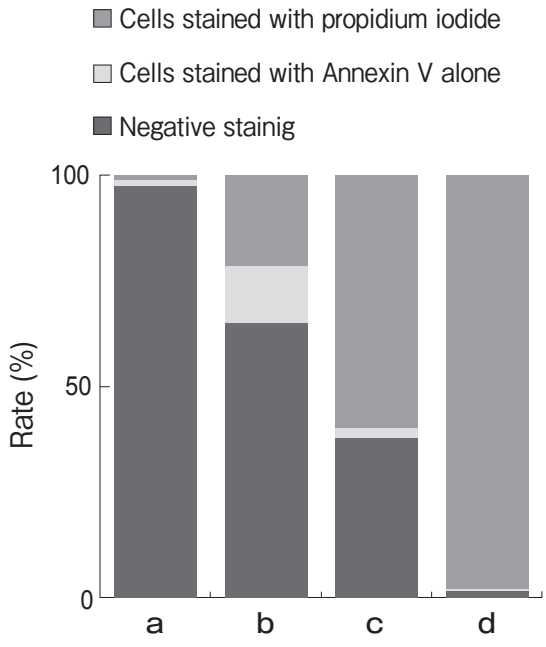

Fig. 3 The staining rate of cells with Annexin V and propidium iodide. The vertical axis indicates the staining rate of cells with Annexin V and propidium iodide. **a**, Non-heated cells; **b**, Cells incubated for 9 h after heating at 42℃; **c**, Cells incubated for 5 h after heating at 48℃; **d**, Cells incubated for 24 h after heating at 48℃.

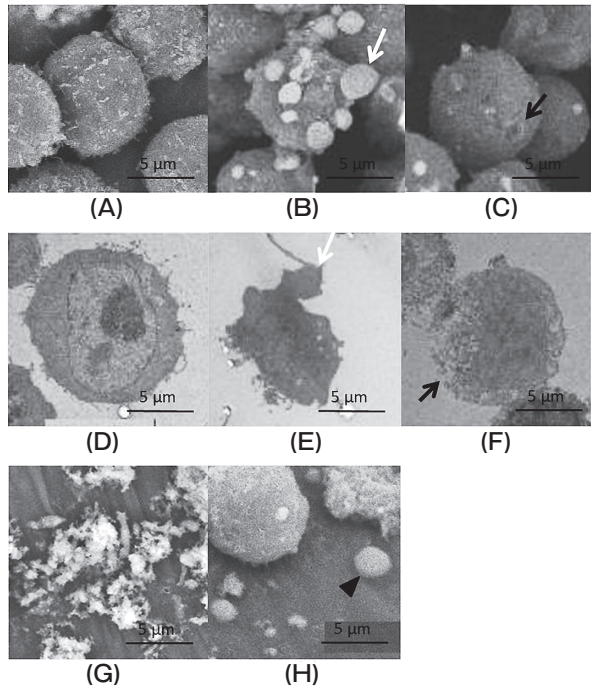

Fig. 4 Changes in cell morphology after heat treatments. (**A**–**C**, **G**, **H**), Cells observed with scanning electron microscope. (**D**–**F**), Cells observed with transmission electron microscope. (**A**) and (**D**), Normal cells. (**B**) and (**E**), Apoptotic cells incubated for 9 h after heating at 42℃. (**C**) and (**F**), Necrotic cells incubated for 24 h after heating at 48℃. (**G**), Sonicated cells. (**H**), Micro-particles. White arrows indicate budding. Black arrows indicate the hole of the cell membrane. The arrow head indicates a micro-particle.

sec, which was about one-third that of normal cells, -1.89×10^{-6}ml mm^2/sec. When cells were heated at 48℃, the ADC values of heated cells increased with the prolongation of post-heating incubation time at 37℃ from 5 h (Fig. 5C) to 24 h (Fig. 5D), compared to those of normal cells (Fig. 5A). The destruction of heated cells by sonication increased the ADC values of cells, when cells were sonicated at 5 h after heating at 48℃ (Fig. 5E). The reduction rate of ADC values of sonicated heated cells as a function of cell density was similar to the rate of sonicated non-heated cells.

The influence of apoptosis. When cells were incubated for 9 h after heating at 42℃, the maximum cell density in the bio-phantom decreased to 5.2×10^8/ml, compared to 1.2×10^9/ml for non-heated cells. When cells were incubated for 9 h after heating at 42℃, the ADC values of cells with densities between 4.5×10^8/ml and 5.2×10^8/ml were between 0.54×10^{-3}mm^2/sec and 1.05×10^{-3}mm^2/sec. Thus, the ADC values of heated cells were lower than those of normal cells at similar densities (Fig. 6). The particle analysis using flow cytometry revealed that the number of micro-particles in the extracellular space among cells increased in the bio-phantom after incubation for 9 h after heating at 42℃. The fraction of micro-particles in bio-phantoms containing heated cells was $21.3\pm12.3\%$, compared to $11.7\pm7.5\%$ in bio-phantoms containing non-heated cells (Fig. 7).

Discussion

Before examining the ADC values of cells in this study, it was examined whether or not the accurate ADC values within the range between 0.59×10^{-3}mm^2/sec and 3.13×10^{-3}mm^2/sec could be accurately measured in a micro cuvette using ADC standard phantoms made by polyethylene glycol [21]. Cell density and cell membrane permeability may be important factors affecting ADC at long diffusion times, although the values of ADC at short diffusion times may be

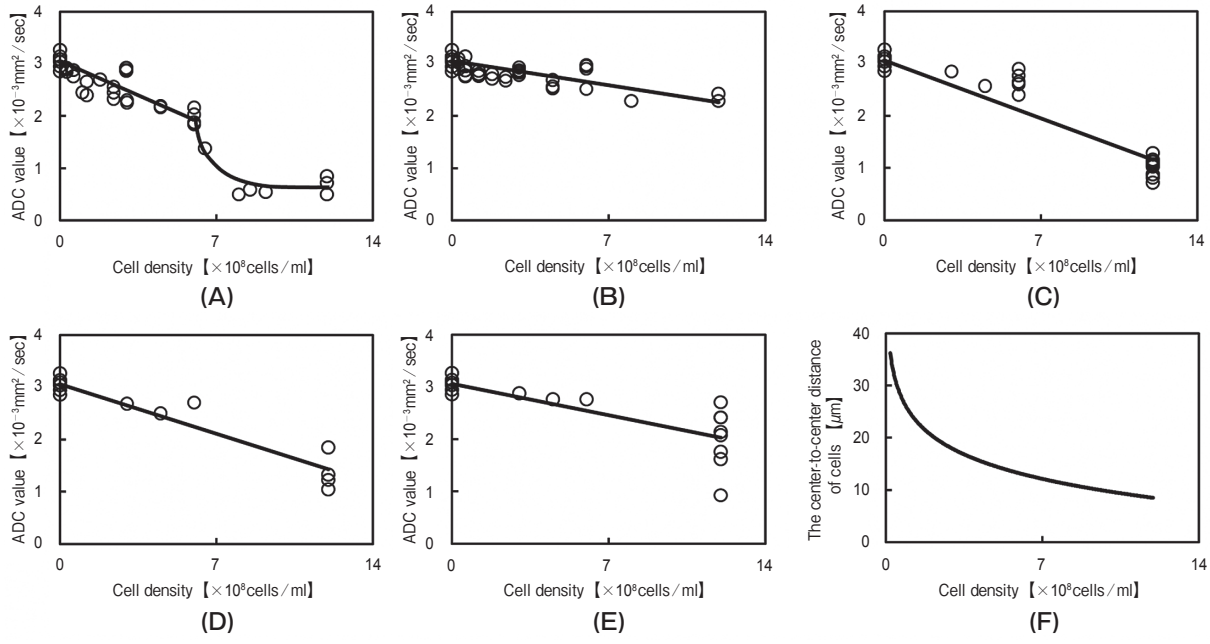

Fig. 5 The ADC values of the bio-phantoms including cells. (**A**) The ADC values of normal cells. (**B**) The ADC values of sonicated normal cells. (**C**) The ADC values of cells incubated for 5h after heating at 48℃. The reduction rate was -1.59×10^{-6}ml mm^2/sec. (**D**) The ADC values of cells incubated for 24h after heating at 48℃. The reduction rate was -1.36×10^{-6}ml mm^2/sec. (**E**) The ADC values of sonicated cells incubated for 5h after heating at 48℃. (**F**) The relationship between cell density and the center-to-center distance of cells. (**A**–**F**) The horizontal axis indicates the cell density. (**A**–**E**) The vertical axis indicates ADC values. (**F**) The vertical axis indicates the center-to-center distance of cells. Straight lines are regression lines to data.

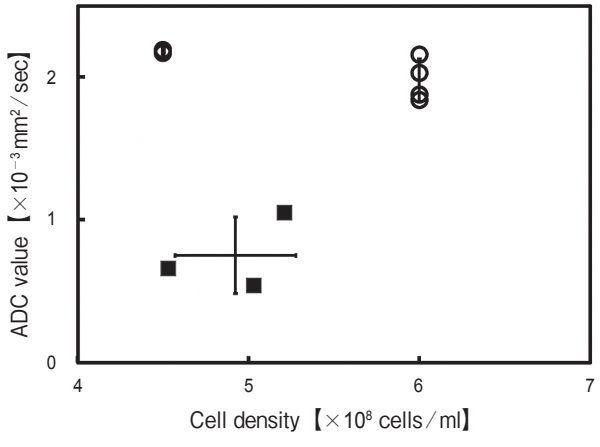

Fig. 6 A comparison of the ADC values between cells incubated for 9h after heating at 42℃ and normal cells. The horizontal axis indicates the cell density. The vertical axis indicates ADC values. Open circles and closed squares indicate the ADC values of normal cells and heated cells, respectively. The vertical and horizontal bars indicate standard deviations.

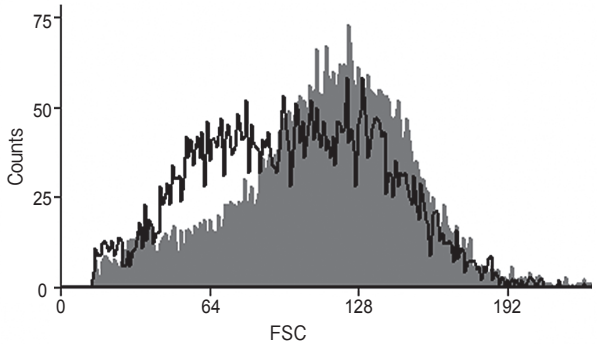

Fig. 7 The increase in micro-particles during apoptosis. The horizontal axis indicates the forward scatter of flow cytometry which correlates with size of cells. The vertical axis indicates the count of cells. Gray, non-heated cells; black line, cells incubated for 9h after heating at 42℃.

influenced strongly by intracellular structures and their changes [22]. In this study, the intermediate constant diffusion time of 30 msec and b values less than 500 sec/mm were used. Under this situation, the signal-noise ratio of DWI was over 3.7. The range of diffusion observable by setup in the diffusion time of 30 msec is larger than the size of the cells, so we think that this setup is satisfactory to measure ADC values made from cells. In this setting, we confirmed the accurate measurement of ADC values of ADC standard phantoms within the range between 0.59×10^{-3} mm^2/sec and 3.13×10^{-3} mm^2/sec.

Lyng *et al.*, examined the relationship between *in vivo* pathological findings of human melanoma transplanted in mice and these ADC values, and reported that ADC values decreased according to the increase in cell density [23]. Stadnic *et al.*, examined *in vivo* pathological findings of a brain tumor and reported that ADC values decreased with decreases in extracellular space [5].

Although cellular ADC values were examined *in vitro* in several reports [2, 10, 13–17], it is impossible to distribute cells uniformly in bio-phantoms without the use of a gel [10] such as that we have developed. There are 2 reports that the cells were arranged three-dimensionally and uniformly with a gel [10, 15]. Anderson *et al.*, [15] investigated the relationship between ADC values and cell volume fraction in cell suspensions using Matrigel™ matrix. As they packed 2 kinds of cells, of different sizes, into gels, the accurate cell density in the gel and accurate size of extracellular space could not be calculated. Most past *in vitro* ADC measurement of cells has been done at temperatures (*e.g.* 20℃ [15]) lower than 37℃, the physiological body temperature. Measurement at low temperature might make it difficult to distinguish between the free diffusion of extracellular space and the restricted diffusion of the intracellular space.

This *in vitro* analysis of ADC measured at 36.5 ± 0.5℃ clarified that ADC values decreased rapidly when the center-to-center distance of cells became less than 13 μm. This means that the ADC values decreased rapidly according to the increase in the restriction of diffusion in the extracellular spaces due to cellular membranes when the distance between cells became less than 3 μm, because the average diameter of Jurkat cells is 9.6 μm [10].

The ADC values of cells increased by sonication. This result was thought to be due to the segmentation of all membrane structures in cells including the cell membrane and nuclear membrane. The reduction rate of ADC values of sonicated cells as a function of cell density was about one-third that of normal cells.

Jurkat cells have been reported to undergo apoptosis and necrosis following heating at 42℃ and 46℃, respectively [19]. In our previous study, we clarified that heating at 42℃ induces apoptosis in Jurkat cells using time-lapse microscopic observation and double staining by AV and PI [19]. The apoptotic DNA fragmentation after heating of Jurkat cells at 42℃ took the "ladder" pattern [19]. In this study, it was confirmed that heating at 42℃ induces apoptosis and heating at 48℃, higher than in the previous report, induces necrosis. Heating at 48℃ induced necrosis in the cells and injured cellular membranes with a resultant increase in ADC values. The proportion of necrotic cells in the bio-phantoms and the resultant ADC values increased according to the prolongation of incubation time after heating. This suggests that the destruction of cellular membranes accompanied with necrosis increased the diffusion of water molecules into intracellular and extracellular spaces. The increase in ADC values after heating at 48℃ was less than the increase in ADC values after sonication. This means the destruction of membrane structures after heating was less than that after sonication. However, the sonication of heated cells increased ADC values to a similar extent to the sonication of non-heated sonicated cells. This indicates that heating at 48℃ might not change the ADC values of the intracellular components.

It has been reported that ADC values increased because necrosis occurred with a resultant decrease in cell density [1, 23–24]. In these *in vivo* reports, it could not be identified which was the main cause for the increase in ADC value, the membrane injury of necrotic cells or the decrease in cell density due to necrosis. In our *in vitro* study, the cell densities in bio-phantoms were adjusted after each heat treatment, and it was clarified that the change of membrane structure itself increases ADC values through observation using electronic microscopes.

Apoptotic cells with budding and micro-particles, which might be apoptotic bodies, increased after heating at 42℃. The maximum cell densities of apoptotic cells in bio-phantoms decreased to approximately half those of non-heated cells due to the increase in micro-

particles among cells. The ADC values of apoptotic cells were lower than these of normal cells at the same density. The decrease in ADC values due to apoptosis might be attributed to the increase in micro-particles in extracellular space. With calculation using data from Fig. 4 and Fig. 5, if micro-particles of 0.47×10^9/ml density exist among cells that are on average $7\,\mu$m apart, the reduction of ADC values would be 1.40×10^{-3}mm^2/sec. Although the ADC reflects physically very different restrictions for different time periods—cytoplasm (and possibly smaller intracellular structures) in the short term and cell membrane permeability in the long term [7–8]—our intermediate diffusion time might reflect the structural change of cells during the apoptotic procedure.

Wendland *et al.* [25] reported that apoptosis occurred due to the hypoxic injury of brain tissues and was decreased in *in vivo* ADC values, although the mechanisms underlying these actions were not identified. This decrease in ADC values during apoptosis might be caused by the blocking of water diffusion into the extracellular spaces by apoptotic bodies. On the other hand, some studies [18, 26–28] have examined *in vivo* tumor tissues and have indicated that the ADC values increased due to apoptosis. The mechanism of increase in ADC values during apoptosis is assumed to be cell shrinkage and a decrease in cell density. Although our *in vitro* results may have limitations in interpreting the entire *in vivo* process of ADC alteration during apoptosis, the significance of this study is that we clarified the role of micro-particles, which increased during apoptosis, in the decrease of ADC values and that we confirmed the importance of extracellular space on ADC values of bio-phantoms.

This *in vitro* study using bio-phantoms was useful for investigating the role of cellular factors and the extracellular space in determining the ADC values yielded by tumor cells and the mechanism of alteration due to apoptosis and necrosis in the ADC values. The intermediate diffusion time of 30 msec might be useful to distinguish between apoptosis and necrosis.

Acknowledgments. We would like to thank the staff of the Department of Radiology and the Central Division of Radiology of Okayama University Hospital for their support on this study. This study was partially supported by Grant-in-Aids for Scientific Research [C (20791516) and C (22591335)] from the Ministry of Health, Labour and Welfare of Japan.

References

1. Koh DM and Collins DJ: Diffusion-weighted MRI in the body: Applications and challenges in oncology. Am J Roentgenol (2007) 188: 1622–1635.
2. Sehy JV, Ackerman JJH and Neil JJ: Apparent diffusion of water, ions, and small molecules in the *Xenopus oocyte* is consistent with Brownian displacement. Magn Reson Med (2002) 48: 42–51.
3. Galons JP, Lope-Piedrafita S, Divijak JL, Corum C, Gillies RJ and Trouard TP: Uncovering of intracellular water in cultured cells. Magn Reson Med (2005) 54: 79–86.
4. Schoeniger JS, Aiken N, Hsu E and Blackband SJ: Relaxation-time and diffusion NMR microscopy of single neurons. J Magn Reson B (1994) 103: 261–273.
5. Stadnik TW, Chaskis C, Michotte A, Shabana WM, van Rompaey K, Luypaert R, Budinsky L, Jellus V and Osteaux M: Diffusion-weighted MR imaging of intracerebral masses: Comparison with conventional MR imaging and histologic findings. Am J Neuroradiol (2001) 22: 969–976.
6. Kilickesmez O, Yirik G, Bayramoglu S, Cimilli T and Aydin S: Non-breath-hold high b-value diffusion-weighted MRI with parallel imaging technique: Apparent diffusion coefficient determination in normal abdominal organs. Diagn Interv Radiol (2008) 14: 83–87.
7. Novikov DS, Fieremans E, Jensen JH and Helpern JA: Random walk with barriers. Nat Phys (2011) 7: 508–514.
8. Novikov DS and Kiselev VG: Effective medium theory of a diffusion-weighted signal. NMR Biomed (2010) 23: 682–697.
9. Tamura T, Usui S, Murakami S, Arihiro K, Akiyama Y, Naito K and Akiyama M: Biexponential signal attenuation analysis of diffusion-weighted imaging of breast. Magn Reson Med Sci (2010) 9: 195–207.
10. Matsumoto Y, Kuroda M, Matsuya R, Kato H, Shibuya K, Oita M, Kawabe A, Matsuzaki H, Asaumi J, Murakami J, Katashima K, Ashida M, Sasaki T, Sei T, Kanazawa S, Mimura S, Oono S, Kitayama T, Tahara S and Inamura K: *In vitro* experimental study of the relationship between the apparent diffusion coefficient and changes in cellularity and cell morphology. Oncol Rep (2009) 22: 641–648.
11. Oliveira JT, Martins L, Picciochi R, Malafaya PB, Sousa RA, Neves NM, Mano JF and Reis RL: Gellan gum: A new biomaterial for cartilage tissue engineering applications. J Biomed Mater Res A (2010) 93: 852–863.
12. Morito A, Fujisawa K, Eguchi T and Ota Y: Protective effects of polysaccharides and polyhydric alcohols in a dry mouth model in cultured cells. Support Care Cancer (2012) 20: 725–731.
13. Sehy JV, Zhao L, Xu J, Rayala HJ, Ackerman JJ and Neil JJ: Effects of physiologic challenge on the ADC of intracellular water in the *Xenopus oocyte*. Magn Reson Med (2004) 52: 239–247.
14. Tanner JE: Intracellular diffusion of water. Arch Biochem Biophys (1983) 224: 416–428.
15. Anderson AW, Xie J, Pizzonia J, Bronen RA, Spencer DD and Gore JC: Effects of cell volume fraction changes on apparent diffusion in human cells. Magn Reson Med (2000) 18: 689–695.
16. Herbst MD and Goldstein JH: A review of water diffusion measurement by NMR in human red blood cells. Am J Physiol (1989) 256: C1097–1104.
17. Roth Y, Ocherashvilli A, Daniels D, Ruiz-Cabello J, Maier SE, Orenstein A and Mardor Y: Quantification of water compartmentation in cell suspensions by diffusion-weighted and T_2-weighted MRI. Magn Reson Imaging (2008) 26: 88–102.
18. Huang MQ, Pickup S, Nelson DS, Qiao H, Xu HN, Li LZ, Zhou R,

Delikatny EJ, Poptani H and Glickson JD: Monitoring response to chemotherapy of non-Hodgkin's lymphoma xenografts by T_2-weighted and diffusion-weighted MRI. NMR Biomed (2008) 21: 1021–1029.
19. Honda O, Kuroda M, Joja I, Asaumi J, Takeda Y, Akaki S, Togami I, Kanazawa S, Kawasaki S and Hiraki Y: Assessment of secondary necrosis of Jurkat cells using a new microscopic system and double staining method with annexin V and propidium iodide. Int J Oncol (2000) 16: 283–288.
20. Hales TC: A proof of the Kepler conjecture. Ann Math (2005) 162: 1065–1185.
21. Matsuya R, Kuroda M, Matsumoto Y, Kato H, Matsuzaki H, Asaumi J, Murakami J, Katashima K, Ashida M, Sasaki T, Sei T, Himei K, Katsui K, Katayama N, Takemoto M, Kanazawa S, Mimura S, Oono S, Kitayama T, Tahara S and Inamura K: A new phantom using polyethylene glycol as an apparent diffusion coefficient standard for MR imaging. Int J Oncol (2009) 35: 893–900.
22. Xu J, Xie J, Jourquin J, Colvin DC, Does MD, Quaranta V and Gore JC: Influence of cell cycle phase on apparent diffusion coefficient in synchronized cells detected using temporal diffusion spectroscopy. Magn Reson Med (2011) 65: 920–926.
23. Lyng H, Haraldseth O and Rofstad EK: Measurement of cell density and necrotic fraction in human melanoma xenografts by diffusion weighted magnetic resonance imaging. Magn Reson Med (2000) 43: 828–836.
24. Ohira T, Okuma T, Matsuoka T, Wada Y, Nakamura K, Watanabe Y and Inoue Y: FDG-microPET and diffusion-weighted MR Image evaluation of early changes after radiofrequency ablation in implanted VX2 tumors in rabbits. Cardiovasc Intervent Radiol (2009) 32: 114–120.
25. Wendland MF, Faustino J, West T, Manabat C, Holtzman DM and Vexler ZS: Early diffusion-weighted MRI as a predictor of caspase-3 activation after hypoxic-ischemic insult in neonatal rodents. Stroke (2008) 39: 1862–1868.
26. Morse DL, Galons JP, Payne CM, Jennings DL, Day S, Xia G and Gillies RJ: MRI-measured water mobility increases in response to chemotherapy via multiple cell-death mechanisms. NMR Biomed (2007) 20: 602–614.
27. Kim H, Morgan DE, Buchsbaum DJ, Zeng H, Grizzle WE, Warram JM, Stockard CR, McNally LR, Long JW, Sellers JC, Forero A and Zinn KR: Early therapy evaluation of combined anti-death receptor 5 antibody and gemcitabine in orthotopic pancreatic tumor xenografts by diffusion-weighted magnetic resonance imaging. Cancer Res (2008) 68: 8369–8376.
28. Huuse EM, Jensen LR, Goa PE, Lundgren S, Anderssen E, Bofin A, Gribbestad IS and Bathen TF: Monitoring the effect of docetaxel treatment in MCF7 xenografts using multimodal *in vivo* and *ex vivo* magnetic resonance methods, histopathology, and gene expression. Transl Oncol (2010) 3: 252–263.